CYCLIC TRIAXIAL TEST OF DYNAMIC SOIL PROPERTIES FOR WIDE STRAIN RANGE

by
Takeji Kokusho(i)

The cyclic triaxial test has been immensely improved in this research so that reliable soil properties corresponding to wide strain range of 10^{-6} to 10^{-3} which are exempt from mechanical frictions of the testing device itself can be readily obtained. A series of cyclic loading tests on a clean sand have yielded the modulus and the damping which are consistent with those obtained by other workers, demonstrating the effectiveness of the test method. Undisturbed sand samples of diluvium have further been tested, showing no significant difference of strain dependency of the modulus and the damping as compared to the specimens made in the laboratory.

INTRODUCTION

Dynamic material properties of soil needed for the nonlinear analysis of earthquake response of the ground have usually been measured in the laboratory using the torsional column shear device, either resonant column type for the strain order of 10^{-5} or less, or the low frequency cyclic loading type for the larger strains. The cyclic triaxial test despite its frequent use in the engineering practice has seldom been looked upon as a rational way to make a reliable measurement of dynamic soil properties for small strain level in particular. The most important reason why the triaxial test has been less authorized as a reasonable means to obtain a good quality dynamic properties seems to come from the difficulties of making reliable measurements corresponding to a smaller strain level than 10^{-4}. Most of the moving parts of the triaxial apparatus suffer from mechanical frictions which make the highly sensitive measurement rather meaningless. In order to obtain reliable soil properties for the small strain range, it is, therefore, essential to eliminate the frictions related with the measurement of displacement and load.

In this experimental research, a highly sensitive displacement sensor which can detect the axial strain as small as 10^{-6} has been introduced just above the loading cap inside the triaxial cell. A sensitive load transducer has also been installed inside the cell to eliminate the effect of the friction of the loading piston. The sketch of the improved triaxial apparatus is shown in Fig. 1. The displacement sensor which is literally free from mechanical friction is composed of two separate electromagnetic discs of 28.6mm in diameter highly sensitive to the relative separation. A pair of sensors have been attached to the both sides of the loading cap as shown in Fig. 1 to detect the average axial displacement killing the component of its uneven movement (Kokusho et al. 1979).

The specimen size was 50mm in diameter and 100mm in height. The specimen was first fully saturated and then isotropically consolidated. The cyclic axial load with the frequency of 0.1Hz or less was applied on the specimen under undrained condition and the hysteresis loops of the axial

(i) Senior Research Engineer, Central Research Institute of Electric Power Industry, JAPAN

stress change vs. the axial strain change were drawn on a chart of a X-Y recorder. On the ground that Possion's ratio ,ν, is almost 0.5 in the undrained situation, shear strain ,γ, and the shear modulus ,G, were derived from axial strain ,ε, and the modulus of deformation ,E.

RESULTS OF CONVENTIONAL TESTS

In order to point out the problems involved in conventional cyclic triaxial tests, a preliminary test was conducted with the apparatus which was equipped with the load cell outside the triaxial chamber and LVDT to measure the axial load and deformation. Fig. 2 shows the shear modulus vs. the logarithm of shear strain relationship for the conventional test. The open circles corresponding to the direct data and the solid circles corresponding to the data modified by taking the effect of the piston friction into consideration tend to dramatically increase as shear strain becomes smaller than 10^{-4}. According to other research works, G vs. logγ curve should be expected to approach to an asymptote with the decrease of γ as shown with the solid curve in Fig. 2. The differences among the three curves indicate the significant effect of the mechanical frictions of not only the loading piston but also the conventional displacment transducer itself on the measured shear modulus in the small strain range.

RESULTS OF IMPROVED TESTS

A number of improved cyclic loading tests were performed for saturated specimen of Toyoura sand (the mean grain size; D_{50} = 0.29mm, the uniformity coefficient; U_c = 1.8). The density of the specimen was controlled by compacting the sand with a handy vibrater. Fig. 3 shows the shear modulus versus shear strain relationships on the semilogarithmic graph obtained from thirteen undrained tests of the dense sand (void ratio e = 0.64) for the confining stresses ranging from 20 to 300KN/m^2. In a clear contrast to the conventional test result, each curve indicates the existence of its asymtotic value as γ becomes smaller. The moduli ,G, normalized by the modulus at $\gamma = 1\times10^{-6}$,G_o, extraporated from the curves in Fig. 3 are taken against logγ in Fig. 4 to obtain the strain dependent curves of the modulus ratio. It is apparent that the average G/G_o vs. logγ curve corresponding to each confining stress moves consistently to the right along γ-axis as the stress becomes higher. Fig. 5 shows the variations of the hysteretic damping ratio ,h, taken against the logarithm of shear strain. Average h versus logγ curves also shift to the right on the graph with the increase of the confining stress.

In Fig. 6, the shear moduli ,G_o, corresponding to $\gamma = 1\times10^{-6}$ obtained by a number of undrained cyclic triaxial tests are plotted against void ratio ,e, to compare with the empirical formula obtained with the resonant column test by Richart et al. (1970) for sands with round grains.

$$G = 7000 \frac{(2.17-e)^2}{1+e} (\sigma_c')^{1/2} \qquad (1)$$

Here, σ_c' is the effective confining stress, and the unit of the stress and the modulus is KN/m^2. The figure indicates that the triaxial test results will coincide well with the formula for all the confining stresses if the multiplier involved in the equation is increased by 20% as illustrated with the dotted curves. This difference of 20% may be attributed to the fact

that for the resonant column test conducted by Harin and Richart (1963) the approximate shear strain level was 3×10^{-5} much larger than 1×10^{-6}. Anyway, it is significant to note that the improved cyclic triaxial test can yield a reliable modulus corresponding to the elastic wave propagation with less efforts than the resonant column test. In Fig. 7 the G/G_o vs. logγ curves obtained in the triaxial test are compared with analogous curves obtained by other workers with the cyclic torsional shear device. Although there exist slight discrepancies among different groups of curves, they are practically in a satisfactory agreement with each other. The strain-dependent variations of the damping ratio measured in this research are compared in Fig. 8 with those given by other workers for clean sands employing other testing apparatus. The improved triaxial test noticiably yields the smallest damping ratio of all. Also obrious is that of all the cyclic tests only the triaxial test yields the damping ratio for the strain smaller than $\gamma = 10^{-4}$ which shows a striking coincidence with that measured by Kuribayashi et al. (1975) using the resonant column device. Quite probably, the existence of mechanical frictions in any cyclic loading test will lead to an apparent increase of the hysteretic damping. Since the stress and strain measurements in the improved triaxial test are completely free from any kind of mechanical frictions, the accuracy of the damping ratio measured in this research should be strongly maintained.

TESTS ON UNDISTURBED SAND SAMPLES OF DILUVIUM

In the preceding section, the efficiency and ease of the improved cyclic triaxial test were demonstrated by comparing the test data for saturated clean sands with other data obtained with other testing devices. The resonant column test which has been playing a key role for measuring the dynamic soil properties of undisturbed soil samples has the limitation in that the strain range to be tested is smaller than 10^{-4}. The cyclic cylindrical torsional shear test which covers the strain up to 10^{-2} can not easily be applicable to undisturbed samples due to the difficulties in sample trimming.

One of the benefits of the improved cyclic triaxial test is that the dynamic properties of the undisturbed soils for the wide range of shear strain can be readily measured. The undisturbed sands tested here were sampled from a diluvial sand layer where the blow counts of SPT were more than 50. The sand samples with the diameter of 84mm were stiff enough to be trimmed with no special procedure to make test specimens. Totally nine specimens picked up at different depths from three boreholes in a certain site were tested. The description of the specimens and their test conditions are listed in Table 1. The sands are relative to very dense and contain very few fines. The specimens first fully saturated by circulating deaired water were isotropically consolidated with effective confining stresses ,σ_c', equal to the insitu mean stresses ,σ_m', which were calculated from the overburden pressures ,σ_v', and the earthpressure coefficient at rest ,K_o, as

$$\sigma_m' = \frac{1+2K_o}{3}\sigma_v' \qquad (2)$$

The average value of K_o was decided to be 0.67 based on the insitu measurement of horizontal earthpressure. In each test Skempton's B coefficient was measured after the application of the back pressure of 200KN/m^2 and confirmed to be more than 0.95.

In Fig. 9, the shear moduli ,G, are plotted against shear strain ,γ, on the G vs. logγ diagram for the nine undisturbed sand specimens. The symbols used in the figure are listed in Table 1. Every curve connecting the plots shows a remarkably smooth change of the modulus within the strain intervals of 10^{-6} to 10^{-3} and clearly indicates the existence of the asymptote as γ becomes infinitely small. The shear moduli ,G, normalized by the modulus at $\gamma = 1\times10^{-6}$,G_o, extraporated by the curves in Fig. 9 for nine tests are plotted against logγ in Fig. 10. The four solid lines drawn in the graph correspond to the analogous curves shown in Fig. 4 obtained for Toyoura sand specimens which were prepared in the laboratory. A brief study of this figure with the help of Table 1 reveals the basic agreement of the strain-dependent variations of the shear modulus ratio between the undisturbed sands and Toyoura sand corresponding to different confining stresses. There exists some slight discrepancy, however, like specimens No. 3 , 4 and 9 in which the shear modulus ratio tends to decrease at a smaller strain level than Toyoura sand, and the cementation effect of the undisturbed diluvial sands may be responsible for this. In Fig. 11 the hysteretic damping ratios measured for the undisturbed sands are plotted against shear strain. The solid curves in the figure represent the analogous relationships shown in Fig. 5 for the specimens of Toyoura sand made in the laboratory. The damping ratios for the undisturbed sands are in a good agreement with those for Toyoura sand for the shear strain ,γ, less than 4×10^{-4} except the strange result of the specimen No. 9 . For larger strains than this, the undisturbed sands give slightly smaller damping ratios than Toyoura sand, implying that the cementation effect may result in smaller hysteretic dampings except for the small strain range.

From the shear modulus at $\gamma = 1\times10^{-6}$,G_o, determined in Fig. 9, the shear wave velocity, V_s, was evaluated using the equation

$$V_s = \sqrt{G/\rho} \qquad (3)$$

where ρ, the density of the soil, was taken as 2.0 to 2.1gr/cm^3 according to the total weight of the saturated sand. In Fig. 12 the shear wave velocities calculated with Eq. (3) are plotted to compare with the results of the insitu seismic downhole survey in the three boreholes. The velocities based on the improved triaxial test on the undistrubed samples undershoot the insitu values by minimum 6 to maximum 33 percent. Although the differences may be explained in several ways, the most probable cause seems to be the disturbance induced in the sand in the process of sampling which may somehow reduce the cementation effect of the dense sand, resulting in the considerable decrease of the elastic shear modulus. Special care should also be taken of the trimming and setting procedures of the specimen so that a weaker part shall not be introduced to the top or bottom end of the specimen.

ACKNOWLEDGEMENT

The author wishes to acknowledge his deep sense of gratitude to professors of Tokyo University, Dr. K. Ishihara and Dr. F. Tatsuoka, as well as Dr. S. Yasuda of Kisojiban Consultants for their valuable suggestions on the dynamic soil test.

REFERENCES

(1) Hardin, B.O. and Drnevich, V.P. (1970), "Shear Modulus and Damping in Soils-I, Measurement and Parameter Effects," Technical Report, Soil Mechanics Series No.1, Dept. of Civil Engineering, University of Kentucky.

(2) Hardin, B.O. and Richart, F.E. (1963), "Elastic Wave Velocities in Granular Soils, "Proc. of ASCE, Vol. 89, SM1, pp 33-65.

(3) Iwasaki, T., Tatsuoka, F. and Takagi, Y. (1976), "Dynamic Shear Deformation Properties of Sand for Wide Strain Range," Report of Public Works Institute No.1085, Ministry of Construction (in Japanese).

(4) Kokusho, T., Sakurai, A. and Esashi, Y. (1979), "Cyclic Triaxial Test of Dynamic Soil Properties for Wide Strain Range," Research Report of Central Research Institute of Electric Power Industry (CRIEPI) No.379002 (in Japanese).

(5) Kuribayashi, E., Iwasaki, T., Tatsuoka, F. and Horiuchi, S. (1974), "Dynamic Deformation Properties of Soils: The Resonant Column Test," Report of Public Works Institute No.912, Ministry of Construction (in Japanese).

(6) Richart, F.E., Hall, J.R. and Woods, R.D. (1970), "Vibration of Soils and Foundations," Prentice-Hall Inc.

(7) Silver, M.L. and Seed, H.B. (1971), "Deformation Characteristics of Sands Under Cyclic Loading," Proc. of ASCE, Vol. 97, SM8, pp 1081-1098.

Spec. No.	Symbols in Fig.9~12	Bore Hole No.	Depth from GL (m)	Dry Unit Weight γ_d (gr/cm³)	Void Ratio e	Mean Grain Size D_{50}(mm)	Uniformity Coefficient U_c	Fine Content (Percent)	Effective Confining Pressure (KN/m²)	Back Press (KN/m²)	B-coefficient
①	▽	1	9.5 ~10.1	1.757	0.565	0.37	1.7	1	105	200	0.96
②	△	1	9.8 ~10.3	1.725	0.594	0.40	1.5	1	107	200	0.98
③	◇	1	18.5 ~19.4	1.629	0.689	0.30	1.9	2	182	200	0.96
④	⊗	1	18.5 ~19.4	1.772	0.552	0.34	2.0	1	182	200	1.00
⑤	○	2	17.0 ~17.6	1.740	0.580	0.42	1.6	1	180	200	1.00
⑥	⊕	2	17.0 ~17.6	1.783	0.542	—	—	—	180	200	0.98
⑦	○	2	20.4 ~21.8	1.660	0.652	0.31	1.7	1	210	200	1.00
⑧	⊕	2	20.4 ~21.8	1.665	0.652	0.30	1.8	1	210	200	0.96
⑨	□	3	7.0 ~7.6	1.629	0.621	—	—	—	81	200	1.00

Table.1 Undisturbed Diluvial Sands and Test Conditions (1 KN/m² ≒ 0.01 kg/cm²)

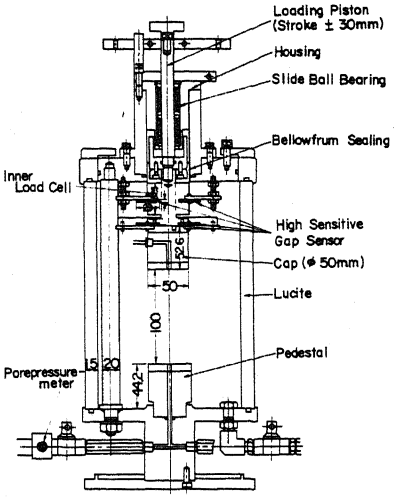

Fig. 1 Triaxial Apparatus Improved to Measure Small Strain Soil Properties.

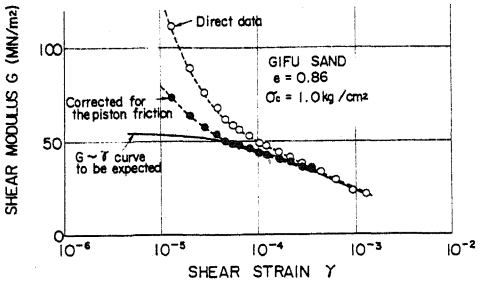

Fig. 2 Shear Modulus vs. Shear Strain Relationships Obtained with the Conventional Triaxial Test. (1 KN/m² ≒ 0.01 kg/cm²)

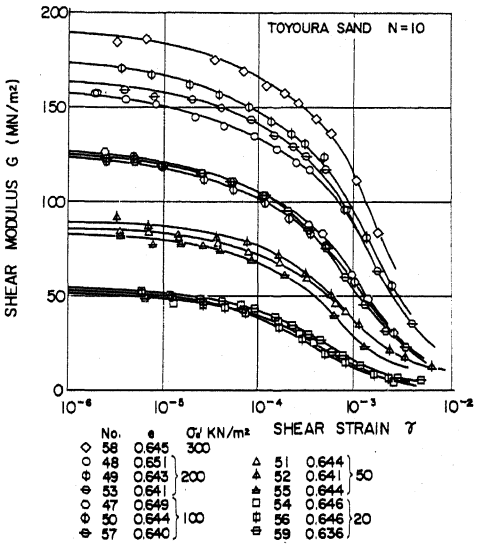

Fig. 3 Shear Modulus vs. Shear Shrain Relationships Obtained, with the Improved Cyclic Triaxal Test. (1 KN/m² ≒ 0.01 kg/cm²)

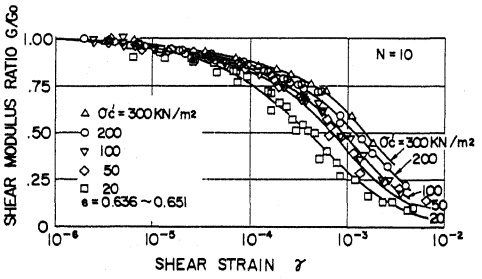

Fig. 4 Shear Modulus Ratio vs. Shear Strain Relationship for Five Confining Stresses. (1 KN/m² ≒ 0.01 kg/cm²)

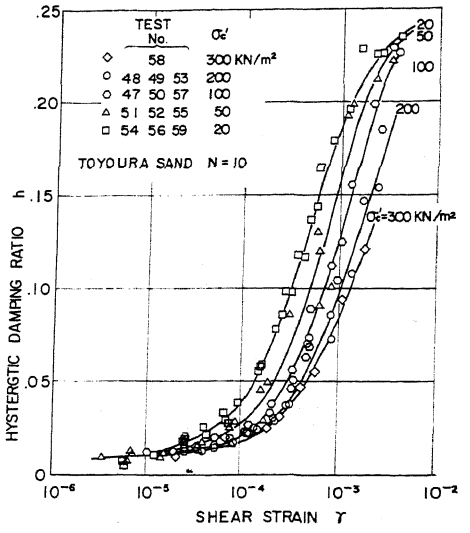

Fig.5 Hysteretic Damping Ratio vs. Shear Stain Relationship for Five Confining Stresses. (1 KN/m² ≒ 0.01 kg/cm²)

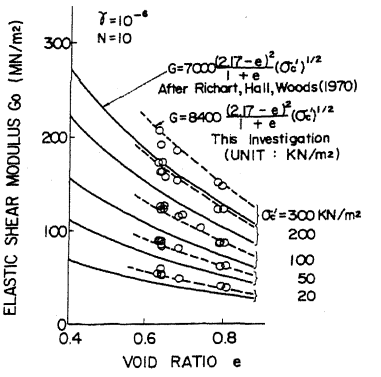

Fig.6 Elastic Shear Modulus vs. Void Ratio Relationship for Five Confining Stresses. (1 KN/m² ≒ 0.01 kg/cm²)

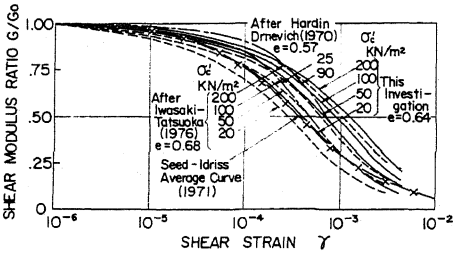

Fig.7 Strain Dependency of Shear Modulus Ratio Compared with Previous Results. (1 KN/m² ≒ 0.01 kg/cm²)

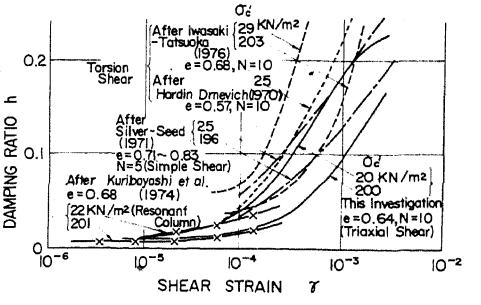

Fig.8 Strain Dependency of Damping Ratio Compared with Previous Results. (1 KN/m² ≒ 0.01 kg/cm²)

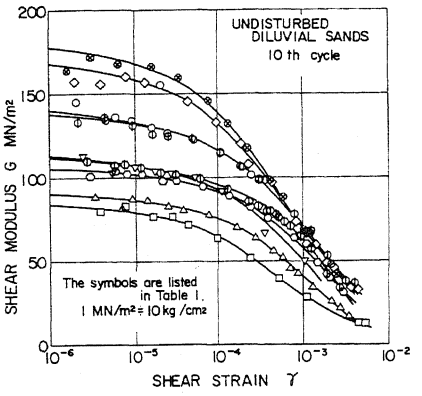

Fig.9 Shear Modulus vs. Shear Strain Relationships for Nine Undisturbed Sand Specimens.

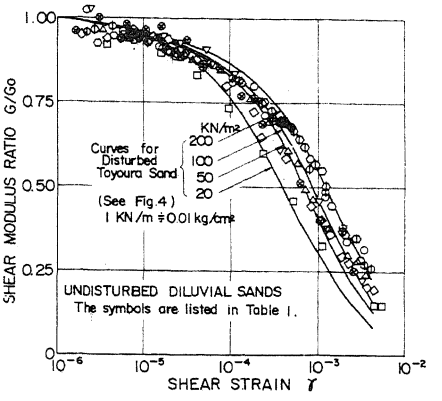

Fig.10 Shear Modulus Ratio vs. Shear Strain Relationships for Undisturbed Sands Compared with Those for Toyoura Sand.

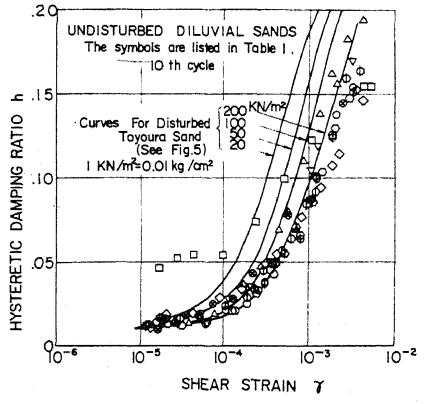

Fig.11 Damping Ratio vs. Shear Strain Relationships for Undisturbed Sands Compared with Those for Toyoura Sand

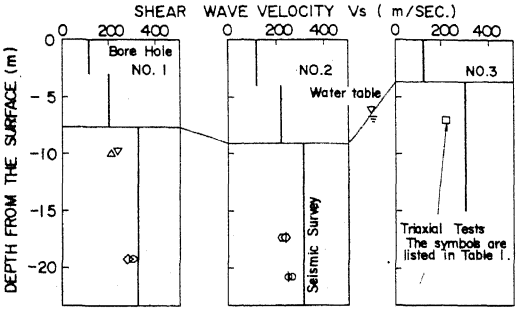

Fig.12 Comparison of Shear Wave Velocities Based on Laboratory tests and Insitu Seismic Survey.